

GLUE: GRADIENT-FREE LEARNING TO UNIFY EXPERTS

Jong-Ik Park*, Shreyas Chaudhari*, Srinivasa Pranav*, Carlee Joe-Wong, and José M. F. Moura

Electrical and Computer Engineering, Carnegie Mellon University

ABSTRACT

In many deployed systems (multilingual ASR, cross-hospital imaging, region-specific perception), multiple pretrained specialist models coexist. Yet, new target domains often require *domain expansion*: a generalized model that performs well beyond any single specialist’s domain. Given such a new target domain, prior works seek a *single* strong initialization prior for the model parameters by first blending expert models to *initialize* a target model. However, heuristic blending—using coefficients based on data size or proxy metrics—often yields *lower target-domain test accuracy*, and learning the coefficients on the target loss typically requires computationally-expensive full backpropagation through the network. We propose **GLUE**, *Gradient-free Learning To Unify Experts*, which initializes the target model as a convex combination of fixed experts, learning the mixture coefficients of this combination via a gradient-free two-point (SPSA) update that requires only two forward passes per step. Across experiments on three datasets and three network architectures, GLUE produces a single prior that can be fine-tuned effectively to outperform baselines. GLUE improves test accuracy by up to **8.5%** over data-size weighting and by up to **9.1%** over proxy-metric selection. GLUE either outperforms backpropagation-based full-gradient mixing or matches its performance within **1.4%**.

Index Terms— Expert Weight Mixing, Model Soup, Gradient-Free Optimization, Two-Point SPSA, Transfer Learning

1. INTRODUCTION

Pretrained parameters, whether from specialist “experts” or large foundation models, enable practitioners to start learning new tasks quickly by *initializing* a target network using the pretrained parameters and then finetuning it on the new task data [1–3]. This practice is commonplace in multilingual or multi-accent automatic speech recognition (ASR) [4], radiology models deployed across scanners and hospitals [5], perception stacks that face region/weather variation [6, 7], recommendation systems partitioned by locale or user segments [8], and foundation model adapters specialized to code, legal, or biomedical text [3, 9, 10]. In these settings, initializing the target network with expert parameters often outperforms knowledge distillation [11, 12], which can introduce optimization noise (e.g., temperature tuning, teacher-student mismatch) and requires extra hyperparameters. In contrast, directly initializing the parameters of the target network with those of the experts simplifies downstream fine-tuning while retaining the pretrained feature hierarchy and inductive biases [13–16].

*Authors contributed equally.

Authors partially supported by NSF Grant CCF-2327905. S. Chaudhari and S. Pranav partially supported by NSF Graduate Research Fellowships (GRFP; Grants DGE1745016, DGE2140739). S. Pranav partially supported by an ARCS Fellowship.

In general, adopting the parameters of a *single* expert is often suboptimal when building a general-purpose model, because real-world data are fragmented across related but distinct distributions [17–19]. Different experts capture complementary structures [20–22], motivating a parameter-space fusion of these experts as an initialization prior. Previous works [23–28] hence seek to *blend* K expert parameters $\{\boldsymbol{\theta}_i\}_{i=1}^K$ as

$$\boldsymbol{\theta}(\boldsymbol{\alpha}) = \sum_{i=1}^K \alpha_i \boldsymbol{\theta}_i, \quad \boldsymbol{\theta}_i \in \mathbb{R}^P \quad (1)$$

where the mixture coefficients $\boldsymbol{\alpha} = (\alpha_1, \dots, \alpha_K)$ define a single deployable model tailored to the target domain.

Common heuristics for finding $\boldsymbol{\alpha}$ include (i) weighting experts by the size of their pretraining data [23], (ii) weighting by an external metric such as held-out accuracy on a proxy dataset [3, 27, 29], or (iii) *learning* the weights by optimizing the target loss [30–32]. Among these, learning the weights $\boldsymbol{\alpha}$ generally leads to the strongest single initialization (prior) for fine-tuning, because it optimizes the true target loss and can capture interactions among experts that global heuristics miss [27, 33].

The practical challenge, however, is cost. Even when the number of mixture weights K is small, standard gradient descent on the mixture coefficients still requires computing the loss gradient $\nabla_{\boldsymbol{\theta}(\boldsymbol{\alpha})}\mathcal{L}$ for the full parameter vector $\boldsymbol{\theta}(\boldsymbol{\alpha})$ of dimension $P \gg K$, thus requiring a complete forward *and* backward pass over the new model.

We propose *Gradient-free Learning to Unify Experts* (**GLUE**), a method for learning expert mixing coefficients $\boldsymbol{\alpha}$ via two-point simultaneous perturbation stochastic approximation (SPSA) [34, 35]. Starting from (1), GLUE optimizes only the low-dimensional vector $\boldsymbol{\alpha}$ [36, 37]. To do so, at each iteration, it samples a random direction $\mathbf{u} \in \mathbb{R}^K$, evaluates the loss at $\boldsymbol{\alpha} \pm \delta\mathbf{u}$ (two forward passes with blended weights $\boldsymbol{\theta}(\boldsymbol{\alpha} \pm \delta\mathbf{u})$), and updates $\boldsymbol{\alpha}$ using the finite-difference estimate. No backpropagation is required—only forward passes—making GLUE lightweight and easy to deploy. While SPSA has been used in other learning tasks, it may be inaccurate in high dimensions [34, 35, 38]. The key insight behind GLUE is that the mixture coefficients are only K -dimensional, mitigating this common drawback of SPSA. Our contributions are threefold:

- **Cost-effective prior construction:** We introduce GLUE, an expert parameter mixing method optimized via two-point SPSA, requiring only forward passes of the blended model.

- **Theory for efficiency and stability:** We derive a per-iteration cost advantage over full-gradient mixing and show how the two-point estimator’s variance scales with the mixture dimension, explaining the stability of low-dimensional updates in GLUE.

- **Empirical validation:** We demonstrate consistent gains of GLUE over existing weighting approaches and competitive performance with full-gradient $\boldsymbol{\alpha}$ optimization, while being far cheaper per iteration; the resulting single prior finetunes effectively on the target domain.

In the following, we review related work (Section 2); introduce **GLUE** and its optimization procedure (Section 3); develop computational and statistical analyses (Section 4); present experiments against baselines (Section 5); discuss practical considerations and limitations (Section 6); and conclude (Section 7).

2. RELATED WORK

A straightforward way to combine experts is to weight each model in proportion to the amount of data used to train it—an idea resembling that of federated averaging (FedAvg), where model updates from multiple clients are aggregated based on clients’ local dataset sizes in order to produce a unified model that (on average) performs well on all clients’ data [23]. While simple and scalable, this strategy is agnostic to the *target* domain. Under distribution changes, such as domain expansion, data-size weighting cannot adapt the mixture to target loss signals and can overemphasize large but misaligned sources.

Another common approach involves choosing or reweighting experts using a proxy metric (e.g., held-out accuracy) and then averaging the expert model parameters. Examples include “model soups”—uniform averaging or greedy selection before averaging—and Fisher-weighted merging, which uses per-parameter Fisher information with model-level mixing as a hyperparameter [3, 27, 29]. These methods can be effective when a reliable proxy set exists, but they decouple weight choice from the training objective and often require manual tuning or discrete selection steps.

A third line of work learns the expert mixture coefficients by minimizing a target-driven objective, ranging from scalar task-vector combinations to interference-aware merging and adaptive (un)supervised schemes that tune model-wise coefficients [30–32]. However, these gradient-based methods require backpropagating through the blended network to compute $\nabla_{\theta(\alpha)} \mathcal{L}$ and then taking inner products with the expert parameters (e.g., $\partial \mathcal{L} / \partial \alpha_i = \langle \nabla_{\theta(\alpha)} \mathcal{L}, \theta_i \rangle$), which is computationally expensive.

Zeroth-order methods replace backpropagation with finite differences. In the two-point SPSA estimator [39], we perturb α along a random direction and estimate a directional derivative with two forward passes, staying in the K -dimensional mixture space where K is the number of experts. However, the estimator’s variance grows with dimension and curvature, demanding many directions or delicate tuning and often causing slow or unstable convergence for large K or ill-conditioned losses [40].

3. METHODOLOGY

In this section, we introduce **GLUE**, *Gradient-free Learning to Unify Experts*, which builds a single prior by mixing fixed experts and learning the mixing parameters α via two-point SPSA.

3.1. Objective

Given K pre-trained expert models with parameters $\{\theta_i\}_{i=1}^K$, we aim to synthesize a *single* pretrained model $\theta(\alpha)$ (defined in (1)) that serves as a strong prior for a *new target domain* that is related to the sources but exhibits a shifted data distribution. Throughout, we *only* optimize the low-dimensional mixing coefficients α ; the expert parameters $\{\theta_i\}_{i=1}^K$ remain fixed.

Let $f(\cdot; \theta)$ denote the network instantiated with parameters θ . For a minibatch $\mathcal{B} = \{(\mathbf{x}_j, \mathbf{y}_j)\}_{j=1}^b$ from the target domain and a standard supervised loss ℓ (cross-entropy for classification or

squared error for regression), we minimize the empirical risk:

$$\mathcal{L}(\alpha) = \frac{1}{b} \sum_{j=1}^b \ell(f(\mathbf{x}_j; \theta(\alpha)), \mathbf{y}_j) \quad (2)$$

We treat α as the sole optimization variable, and employ a zeroth-order (two-point) update on α .

3.2. Two-point SPSA updates

Because our optimization variable is the K -dimensional mixture, and zeroth-order estimates are accurate in lower dimensions [34, 35, 38], we estimate the gradient of \mathcal{L} with respect to α using a two-point simultaneous perturbation.

At each iteration, we draw a random direction vector $\mathbf{u} \in \mathbb{R}^K$ (e.g., by drawing entries of \mathbf{u} i.i.d. from a Gaussian or Rademacher distribution and normalizing) and choose a small radius $\mu > 0$. We form perturbed unconstrained coefficients $\alpha_{\pm} = \alpha \pm \mu \mathbf{u}$ and corresponding blended parameters $\theta(\alpha_{\pm}) = \sum_{i=1}^K \alpha_{\pm i} \theta_i$. At both blends, we then evaluate the loss on the same minibatch of target-domain examples, keeping inference deterministic across the two probes (e.g., BatchNorm in evaluation mode and fixed randomness) so that differences reflect only the perturbation:

$$L_{\pm} = \frac{1}{b} \sum_{j=1}^b \ell(f(\mathbf{x}_j; \theta(\alpha_{\pm})), \mathbf{y}_j) \quad (3)$$

The directional finite difference along \mathbf{u} is

$$d(\alpha; \mathbf{u}) = \frac{L_{+} - L_{-}}{2\mu} \quad (4)$$

which induces the Gaussian-smoothing gradient estimate

$$\hat{\nabla}_{\alpha} \mathcal{L}(\alpha) = d(\alpha; \mathbf{u}) \mathbf{u} \quad (5)$$

When desired, we can reduce variance by additionally averaging over m independently sampled directions $\{\mathbf{u}_r\}_{r=1}^m$ in the same iteration,

$$\hat{\nabla}_{\alpha} \mathcal{L}(\alpha) = \frac{1}{m} \sum_{r=1}^m \frac{L_{+}^{(r)} - L_{-}^{(r)}}{2\mu} \mathbf{u}_r \quad (6)$$

with \mathbf{u}_r sampled as above and $L_{\pm}^{(r)}$ computed as in (3). Finally, we update the mixture parameters:

$$\alpha \leftarrow \alpha - \eta \hat{\nabla}_{\alpha} \mathcal{L}(\alpha) \quad (7)$$

where $\eta > 0$ is the step size. In our experiments, we perform SPSA and momentum updates in the unconstrained β -space and map to $\alpha = \text{softmax}(\beta)$, replacing (7). Optimizing in β ensures that $\theta(\alpha)$ remains within the convex hull of the expert parameters.

3.3. From mixture to prior

We initialize $\alpha = \frac{1}{K} \mathbf{1}$ and iterate the two-point updates over minibatches until validation performance plateaus. Formally, we target the empirical-risk minimizer and then map it to a single blended model:

$$\alpha^* \in \underset{\alpha \in \mathbb{R}^K}{\text{argmin}} \mathcal{L}(\alpha), \quad \theta^* = \theta(\alpha^*) \quad (8)$$

The resulting θ^* serves as the starting point for standard gradient-based adaptation on the target domain, providing a strong prior that concentrates the most relevant inductive biases from the experts.

4. THEORETICAL ANALYSIS

In this section, we show that the two-point (SPSA) procedure used in GLUE is (i) computationally cheaper per iteration than gradient-based mixing and (ii) statistically stable when the mixture dimension K (the number of experts) is sufficiently small. To do so, we leverage results in stochastic approximation and zeroth-order optimization [34, 35, 38].

4.1. Two-point (SPSA) vs. full-gradient cost for updating α

We compare a single SPSA step on α with a full-gradient step on α when the model parameters are blended as $\theta(\alpha) = \sum_{i=1}^K \alpha_i \theta_i$ and the experts $\{\theta_i\}_{i=1}^K$ are fixed.

Let F denote the cost of one forward pass of the blended network on the current minibatch, and let the cost of a full backward pass be γF with $\gamma \geq 2$ (typical for deep neural networks [41]). Let C_{mix} be the cost of the multiply-accumulate operations used to form a blended parameter vector $\theta(\alpha)$ from the K experts: $C_{\text{mix}} = O(PK)$ memory operations for parameter dimension P . Let D_α be the cost of computing the gradient $\nabla_\alpha \mathcal{L} = [\langle \nabla_{\theta(\alpha)} \mathcal{L}, \theta_1 \rangle, \dots, \langle \nabla_{\theta(\alpha)} \mathcal{L}, \theta_K \rangle]$ given $\nabla_{\theta(\alpha)} \mathcal{L}$, which is an $O(PK)$ dot-product accumulation. Evaluating $\nabla_\alpha \mathcal{L}$ at the current mixture requires (i) computing $\theta(\alpha)$ once, (ii) one forward pass and one backward pass to compute $\nabla_{\theta(\alpha)} \mathcal{L}$, and (iii) D_α for computing K inner products with $\langle \nabla_{\theta(\alpha)} \mathcal{L}, \theta_i \rangle$. With one perturbation pair ($m = 1$), SPSA evaluates the loss at two nearby mixtures $\alpha_\pm = \alpha \pm \delta \mathbf{u}$, requiring two blends and two forwards, but *no* backward. Therefore:

$$T_{\text{full}} = (1 + \gamma)F + C_{\text{mix}} + D_\alpha, \quad T_{\text{SPSA}} = 2(F + C_{\text{mix}}) \quad (9)$$

Whenever $T_{\text{SPSA}} < T_{\text{full}}$, SPSA is cheaper than the full-gradient step. Therefore, whenever

$$C_{\text{mix}} < (\gamma - 1)F + D_\alpha \quad (10)$$

a single SPSA pair is cheaper than a full-gradient step. In practice, the condition is easily met since (i) the inner product cost D_α is typically of the same order as the mixing cost C_{mix} and (ii) the cost of the backward pass is typically more than $2F$ ($\gamma \geq 2$).

4.2. Variance of two-point estimates

We analyze the variance of the two-point (SPSA) gradient estimator $\bar{\mathbf{g}}(\alpha)$, an average over m i.i.d. random direction vectors $\{\mathbf{u}_r\}_{r=1}^m$:

$$\bar{\mathbf{g}}(\alpha) = \frac{1}{m} \sum_{r=1}^m \hat{\mathbf{g}}(\alpha; \mathbf{u}_r) \quad (11)$$

$$\hat{\mathbf{g}}(\alpha; \mathbf{u}) = \left(\frac{\mathcal{L}(\alpha + \mu \mathbf{u}) - \mathcal{L}(\alpha - \mu \mathbf{u})}{2\mu} \right) \mathbf{u}, \quad \mu > 0 \quad (12)$$

Let $\mathbf{g} = \nabla_\alpha \mathcal{L}$ denote the true gradient of the loss with respect to α . As $\mu \rightarrow 0$, $\hat{\mathbf{g}}$ becomes the directional derivative of \mathcal{L} with respect to \mathbf{u} and the approximation error scales with the square of μ : $\hat{\mathbf{g}} = (\mathbf{g}^\top \mathbf{u}) \mathbf{u} + O(\mu^2)$. Since the directional derivative is an unbiased estimator of \mathbf{g} , both $\hat{\mathbf{g}}$ and $\bar{\mathbf{g}}$ are also unbiased [42]. Therefore, we bound the variance of $\bar{\mathbf{g}}$ in the following proposition—where the variance refers to the trace of the covariance matrix of the averaged gradient estimator $\bar{\mathbf{g}}$.

Proposition 1 (Variance Bound). *The variance of the two-point (SPSA) gradient estimator $\bar{\mathbf{g}}(\alpha)$ is upper bounded as:*

$$\mathbb{E} [\|\bar{\mathbf{g}} - \mathbf{g}\|^2] \leq \frac{K-1}{mK} \sigma_{\max}(\Theta)^2 \|\nabla_\theta \mathcal{L}\|^2 + O(\mu^2) \quad (13)$$

where $\Theta = [\theta_1, \theta_2, \dots, \theta_K]$ and $\theta = \Theta \alpha$.

Proof. We consider the first order Taylor approximation of (12):

$$\hat{\mathbf{g}}(\alpha; \mathbf{u}) = (\mathbf{g}^\top \mathbf{u}) \mathbf{u} + O(\mu^2) \quad (14)$$

We proceed to compute $\mathbb{E} [\|\hat{\mathbf{g}} - \mathbf{g}\|^2]$ by using the fact that \mathbf{u} being a unit isotropic random vector implies $\|\mathbf{u}\| = 1$ and $\mathbb{E}[\mathbf{u} \mathbf{u}^\top] = \frac{1}{K} \mathbf{I}$.

$$\mathbb{E} [\|\hat{\mathbf{g}} - \mathbf{g}\|^2] = \mathbb{E} \left[\left\| (\mathbf{g}^\top \mathbf{u}) \mathbf{u} + O(\mu^2) - \mathbf{g} \right\|^2 \right] \quad (15)$$

$$= \mathbb{E} \left[\left\| (\mathbf{g}^\top \mathbf{u}) \mathbf{u} \right\|^2 - 2(\mathbf{g}^\top \mathbf{u})^2 \right] + \|\mathbf{g}\|^2 + O(\mu^2) \quad (16)$$

$$= -\mathbf{g}^\top \mathbb{E} [\mathbf{u} \mathbf{u}^\top] \mathbf{g} + \|\mathbf{g}\|^2 + O(\mu^2) \quad (17)$$

$$= \frac{K-1}{K} \|\mathbf{g}\|^2 + O(\mu^2) \quad (18)$$

The variance with respect to $\bar{\mathbf{g}}$ is then:

$$\text{Var}[\bar{\mathbf{g}}] = \frac{1}{m} \text{Var}[\hat{\mathbf{g}}] = \frac{K-1}{mK} \|\mathbf{g}\|^2 + O(\mu^2) \quad (19)$$

We proceed to bound $\|\mathbf{g}\|^2$ as:

$$\|\mathbf{g}\|^2 = \|\nabla_\alpha \mathcal{L}\|^2 = \|\Theta \nabla_\theta \mathcal{L}\|^2 \leq \sigma_{\max}(\Theta)^2 \|\nabla_\theta \mathcal{L}\|^2 \quad (20)$$

Substituting the inequality above into (19) completes the proof. \square

The proposition demonstrates that if $\sigma_{\max}(\Theta)$ is small, e.g., the expert parameters are more aligned, the variance grows slower in the number of experts K . The variance can be reduced with additional random direction samples (increasing m). Additionally assuming Lipschitz smoothness in the loss function \mathcal{L} with respect to θ can be used to further upper bound $\|\nabla_\theta \mathcal{L}(\theta)\|^2$.

5. EXPERIMENTAL EVALUATIONS

We evaluate GLUE on CIFAR-10, SVHN, and Imagenette using three backbones: ResNet-20, MobileNetV2, and an 8-layer ViT (patch size 8) respectively. We train $K = 10$ expert models on heterogeneous splits of the base dataset. We adopt a non-IID experimental evaluation setup commonly used for federated learning: we sample per-class proportions for each expert from a Dirichlet distribution with concentration parameter $\delta = 0.5$, then subsample a total of 2000 images to match those class proportions. In general, $\delta \leq 0.5$ induces skewed (non-IID) splits; larger δ approaches IID. Each expert is trained for 40 epochs with a batch size of 64 and an Adam optimizer with a learning rate of 0.001 and momentum parameters (0.9, 0.999). After training the experts, we evaluate four methods for determining α , the mixture coefficients used to combine the expert models' parameters:

- **Config 1 (Data-size):** $\alpha_i \propto n_i$, the size of expert i 's pre-training dataset.
- **Config 2 (Proxy-accuracy):** $\alpha_i \propto \text{Acc}_i$, the accuracy of expert i on a small held-out validation set from the target domain.

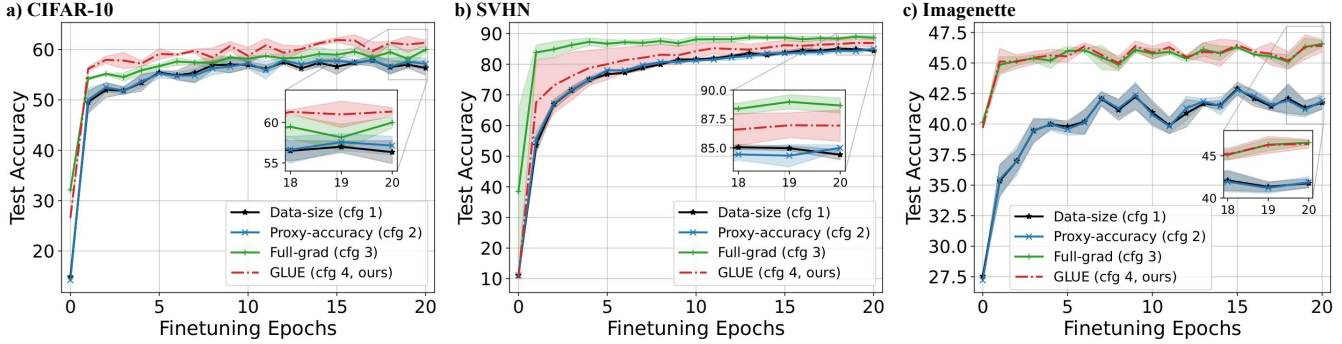


Fig. 1. Fine-tuning test accuracy vs. lightweight finetuning epochs (with fixed α). Datasets: **(a)** CIFAR-10, **(b)** SVHN, **(c)** Imagenette. We compare Configs 1-4 (see Sec. 5). GLUE (Config 4; ours) shows similar trends to Config 3 and consistently achieves higher test accuracy and faster convergence than Configs 1-2.

Table 1. Test accuracies (%) of the 10 experts evaluated on the target training dataset. We bolded the highest/lowest accuracies per row.

Expert	0	1	2	3	4	5	6	7	8	9
CIFAR-10	38.60	47.62	50.45	37.56	46.36	38.80	40.33	39.41	42.92	45.10
SVHN	60.10	71.79	77.05	69.35	70.97	55.82	54.38	60.54	54.96	76.49
Imagenette	33.04	34.06	40.51	29.73	39.49	33.89	32.08	32.94	32.99	38.14

- **Config 3 (Full-grad α):** Learn α by minimizing the target training loss with full backpropagation through $\theta(\alpha)$; we parameterize α and use the same mini-batch schedule as GLUE.
- **Config 4 (GLUE):** Learn α using two-point SPSA on α , requiring only forward evaluations (Sec. 3).

Configs 1 and 2 do not optimize on the target domain; Configs 3 and 4 learn α using target-domain training data. In Configs 3 and 4, we use Adam optimizer with learning rate 1e-2, momentum parameters (0.9, 0.99) to update α . Throughout training, α is constrained to lie in convex hull (i.e., $\sum_i \alpha_i = 1$). Additionally, for GLUE we update α by randomly sampling only *one* random direction u . We use 10000 images sampled IID from the base dataset to learn the unification parameters α and finetune the models as described below. All unified models are subsequently evaluated on the original testing split of each of the base datasets.

After determining α , we form the unified initialization $\theta(\alpha)$ for the target model and report: (i) *prior (zero-shot)* performance of $\theta(\alpha)$ without any target training, and (ii) *finetuned* performance after updating all network parameters on the target training set while *keeping α fixed*. We also report the test accuracy of the *individual experts* before blending in Table 1 for reference. Except for the testing accuracy of experts in Table 1, we ran the experiments with three different random seeds and report the averaged test accuracy.

Figure 1 plots test accuracy during fine-tuning for the four configurations. Across all datasets and backbones, GLUE (Config 4) consistently outperforms data-size weighting (Config 1) by up to **6.7%** on CIFAR-10, **3.8%** on SVHN, and **8.5%** on Imagenette. GLUE also outperforms proxy-accuracy weighting (Config 2) by up to **7.0%** on CIFAR-10, **3.9%** on SVHN, and **9.1%** on Imagenette. GLUE attains similar performance to full-grad α (Config 3): GLUE outperforms full-grad on CIFAR-10 by up to **4.5%** and has at most **1.4%** and **0.5%** variation in test accuracy on SVHN and Imagenette, respectively. To minimize computational cost in these experiments, GLUE computes only one two-point estimate to approximate the gradient at each iteration ($m = 1$). However, the variation in test accuracy between GLUE and full-grad α (Config 3) can be reduced by averaging multiple two-point estimates to obtain better

approximations to the true gradient—as in (6).

In summary, Figure 1 shows that GLUE (Config 4) starts from a stronger prior and converges faster to a higher test accuracy than the alternatives, closely tracking the performance of the full-gradient method (Config 3).

These results highlight that **1)** the performance gains from learning α persist even after finetuning the target model and **2)** GLUE mimics the gains of full-gradient α learning while providing computational benefits by relying only on forward evaluations instead of costly backpropagation.

6. DISCUSSION

In **GLUE**, each step forms two blends and runs two forward passes; there is no backward pass. The per-step cost advantage over full-gradient mixing follows from

$$T_{\text{full}} - T_{\text{SPSA}} = (1 + \gamma)F + C_{\text{mix}} + D_{\alpha} - 2(F + C_{\text{mix}}) = (\gamma - 1)F - C_{\text{mix}} + D_{\alpha} \quad (21)$$

As networks grow, the backward term $(\gamma - 1)F$ dominates, so the gap widens in favor of SPSA. In practice, we also amortize C_{mix} by caching the two blended parameter sets across the paired forward passes.

In this work, GLUE assumes that the architectures are compatible, meaning they share backbones and heads. When the heads differ, we mix the backbone and select or align a single head, optionally refreshing the BatchNorm statistics.

Other limitations include the convex-hull restriction (the target optimum may lie outside the experts' span), possible misalignment across experts (objectives or preprocessing), hyperparameter sensitivity of SPSA (too large radius μ of (6) biases the estimate; too small increases noise), and variance growing with K . These can be mitigated by light calibration, averaging a few directions, or modest schedules, but remain trade-offs.

7. CONCLUSION

We presented **GLUE**, a forward-only approach that learns a single deployable prior by convexly mixing pretrained experts and optimizing the mixture via two-point SPSA. The method avoids backpropagation and is accompanied by cost and variance analyses that explain its efficiency and stability. Empirically, GLUE delivers consistent improvements over data-size weighting and proxy-metric baselines while remaining lightweight to deploy compared to the learned full gradient mixing baseline.

8. REFERENCES

[1] Mehdi Noroozi, Ananth Vinjimoor, Paolo Favaro, and Hamed Pirsiavash, “Boosting self-supervised learning via knowledge transfer,” in *Proceedings of the IEEE Conference on Computer Vision and Pattern Recognition*, 2018, pp. 9359–9367.

[2] Kaichao You, Yong Liu, Jianmin Wang, and Mingsheng Long, “Logme: Practical assessment of pre-trained models for transfer learning,” in *International Conference on Machine Learning*. PMLR, 2021, pp. 12133–12143.

[3] Jong-Ik Park, Srinivasa Pranav, José M.F. Moura, and Carlee Joe-Wong, “Fedbat: Federated learning aggregation biased by a foundation model,” in *International Conference on Artificial Intelligence and Statistics*. PMLR, 2025, pp. 676–684.

[4] Mehmet Ali Tugtekin Turan, Emmanuel Vincent, and Denis Joutet, “Achieving multi-accent asr via unsupervised acoustic model adaptation,” in *INTERSPEECH 2020*, 2020.

[5] Sina Akbarian, Laleh Seyyed-Kalantari, Farzad Khalvati, and Elham Dolatabadi, “Evaluating knowledge transfer in the neural network for medical images,” *IEEE Access*, vol. 11, pp. 85812–85821, 2023.

[6] Yang Shu, Zhangjie Cao, Ziyang Zhang, Jianmin Wang, and Mingsheng Long, “Hub-pathway: transfer learning from a hub of pre-trained models,” *Advances in Neural Information Processing Systems*, vol. 35, pp. 32913–32927, 2022.

[7] Sankar Kumar Pal and Debasree Dutta, “Transfer learning in weather prediction: Why, how, and what should,” *Journal of Computational and Cognitive Engineering*, vol. 3, no. 4, pp. 324–347, 2024.

[8] Junchen Fu, Fajie Yuan, Yu Song, Zheng Yuan, Mingyue Cheng, Shenghui Cheng, Jiaqi Zhang, Jie Wang, and Yunzhu Pan, “Exploring adapter-based transfer learning for recommender systems: Empirical studies and practical insights,” in *Proceedings of the 17th ACM International Conference on Web Search and Data Mining*, 2024, pp. 208–217.

[9] Yang Yuan, “On the power of foundation models,” in *International Conference on Machine Learning*. PMLR, 2023, pp. 40519–40530.

[10] Ce Zhou, Qian Li, Chen Li, Jun Yu, Yixin Liu, Guangjing Wang, Kai Zhang, Cheng Ji, Qiben Yan, Lifang He, et al., “A comprehensive survey on pretrained foundation models: A history from bert to chatgpt,” *International Journal of Machine Learning and Cybernetics*, pp. 1–65, 2024.

[11] Geoffrey Hinton, Oriol Vinyals, and Jeff Dean, “Distilling the knowledge in a neural network,” *arXiv preprint arXiv:1503.02531*, 2015.

[12] Shreyas Chaudhari and José M.F. Moura, “Knowledge distillation by compressive sampling,” in *2023 57th Asilomar Conference on Signals, Systems, and Computers*. IEEE, 2023, pp. 882–886.

[13] Sergey Zagoruyko and Nikos Komodakis, “Paying more attention to attention: Improving the performance of convolutional neural networks via attention transfer,” *arXiv preprint arXiv:1612.03928*, 2016.

[14] Paul Micaelli and Amos J Storkey, “Zero-shot knowledge transfer via adversarial belief matching,” *Advances in Neural Information Processing Systems*, vol. 32, 2019.

[15] Seyed Iman Mirzadeh, Mehrdad Farajtabar, Ang Li, Nir Levine, Akihiro Matsukawa, and Hassan Ghasemzadeh, “Improved knowledge distillation via teacher assistant,” in *Proceedings of the AAAI Conference on Artificial Intelligence*, 2020, vol. 34, pp. 5191–5198.

[16] Amir Moslemi, Anna Briskina, Zubeka Dang, and Jason Li, “A survey on knowledge distillation: Recent advancements,” *Machine Learning with Applications*, vol. 18, pp. 100605, 2024.

[17] Benjamin Cohen-Wang, Joshua Vendrow, and Aleksander Madry, “Ask your distribution shift if pre-training is right for you,” *Transactions on Machine Learning Research*, 2024.

[18] Yuge Shi, Imant Daunhawer, Julia E Vogt, Philip Torr, and Amartya Sanyal, “How robust are pre-trained models to distribution shift?,” in *ICML 2022: Workshop on Spurious Correlations, Invariance and Stability*, 2022.

[19] Liuyu Xiang, Guiguang Ding, and Jungong Han, “Learning from multiple experts: Self-paced knowledge distillation for long-tailed classification,” in *European Conference on Computer Vision*. Springer, 2020, pp. 247–263.

[20] Fei Yuan, Linjun Shou, Jian Pei, Wutao Lin, Ming Gong, Yan Fu, and Dixin Jiang, “Reinforced multi-teacher selection for knowledge distillation,” in *Proceedings of the AAAI Conference on Artificial Intelligence*, 2021, vol. 35, pp. 14284–14291.

[21] Chuhuan Wu, Fangzhao Wu, and Yongfeng Huang, “One teacher is enough? pre-trained language model distillation from multiple teachers,” in *Findings of the Association for Computational Linguistics: ACL-IJCNLP 2021*, 2021, pp. 4408–4413.

[22] Andrei Boiarov, Kostiantyn Khabarlak, and Igor Yastrebov, “Simultaneous perturbation method for multi-task weight optimization in one-shot meta-learning,” in *International Conference on Neural Information Processing*. Springer, 2022, pp. 373–384.

[23] Brendan McMahan, Eider Moore, Daniel Ramage, Seth Hampson, and Blaise Aguera y Arcas, “Communication-efficient learning of deep networks from decentralized data,” in *International Conference on Artificial Intelligence and Statistics*. PMLR, 2017, pp. 1273–1282.

[24] Srinivasa Pranav and José M.F. Moura, “Peer-to-peer learning+consensus with non-iid data,” in *2023 57th Asilomar Conference on Signals, Systems, and Computers*, 2023, pp. 709–713.

[25] Srinivasa Pranav and José M. F. Moura, “Peer-to-peer deep learning for beyond-5g iot,” in *2024 58th Asilomar Conference on Signals, Systems, and Computers*, 2024, pp. 1000–1004.

[26] Shreyas Chaudhari, Srinivasa Pranav, Emile Anand, and José M. F. Moura, “Peer-to-peer learning dynamics of wide neural networks,” in *ICASSP 2025 - 2025 IEEE International Conference on Acoustics, Speech and Signal Processing (ICASSP)*, 2025, pp. 1–5.

[27] Mitchell Wortsman, Gabriel Ilharco, Samir Ya Gadre, Rebecca Roelofs, Raphael Gontijo-Lopes, Ari S Morcos, Hongseok Namkoong, Ali Farhadi, Yair Carmon, Simon Kornblith, et al., “Model soups: averaging weights of multiple fine-tuned models improves accuracy without increasing inference time,” in *International Conference on Machine Learning*. PMLR, 2022, pp. 23965–23998.

[28] Changlong Shi, He Zhao, Bingjie Zhang, Mingyuan Zhou, Dandan Guo, and Yi Chang, “Fedawa: Adaptive optimization of aggregation weights in federated learning using client vectors,” in *Proceedings of the IEEE Conference on Computer Vision and Pattern Recognition*, 2025, pp. 30651–30660.

[29] Michael S Matena and Colin A Raffel, “Merging models with fisher-weighted averaging,” *Advances in Neural Information Processing Systems*, vol. 35, pp. 17703–17716, 2022.

[30] Gabriel Ilharco, Marco Tulio Ribeiro, Mitchell Wortsman, Ludwig Schmidt, Hannaneh Hajishirzi, and Ali Farhadi, “Editing models with task arithmetic,” in *The Eleventh International Conference on Learning Representations*, 2023.

[31] Prateek Yadav, Derek Tam, Leshem Choshen, Colin A Raffel, and Mohit Bansal, “Ties-merging: Resolving interference when merging models,” *Advances in Neural Information Processing Systems*, vol. 36, pp. 7093–7115, 2023.

[32] Enneng Yang, Zhenyi Wang, Li Shen, Shiwei Liu, Guibing Guo, Xingwei Wang, and Dacheng Tao, “Adamerging: Adaptive model merging for multi-task learning,” in *The Twelfth International Conference on Learning Representations*, 2024.

[33] Siyuan Mu and Sen Lin, “A comprehensive survey of mixture-of-experts: Algorithms, theory, and applications,” *arXiv preprint arXiv:2503.07137*, 2025.

[34] Payman Sadegh and James C Spall, “Optimal random perturbations for stochastic approximation using a simultaneous perturbation gradient approximation,” *IEEE Transactions on Automatic Control*, vol. 43, no. 10, pp. 1480–1484, 2002.

[35] Bin Gu, Xiyuan Wei, Shangqian Gao, Ziran Xiong, Cheng Deng, and Heng Huang, “Black-box reductions for zeroth-order gradient algorithms to achieve lower query complexity,” *Journal of Machine Learning Research*, vol. 22, no. 170, pp. 1–47, 2021.

[36] Robert A Jacobs, Michael I Jordan, Steven J Nowlan, and Geoffrey E Hinton, “Adaptive mixtures of local experts,” *Neural Computation*, vol. 3, no. 1, pp. 79–87, 1991.

[37] Hanxiao Liu, Karen Simonyan, and Yiming Yang, “Darts: Differentiable architecture search,” in *International Conference on Learning Representations*, 2019.

[38] Yurii Nesterov and Vladimir Spokoiny, “Random gradient-free minimization of convex functions,” *Foundations of Computational Mathematics*, vol. 17, no. 2, pp. 527–566, 2017.

[39] James C Spall, “Multivariate stochastic approximation using a simultaneous perturbation gradient approximation,” *IEEE Transactions on Automatic Control*, vol. 37, no. 3, pp. 332–341, 2002.

[40] Yan Zhang, Yi Zhou, Kaiyi Ji, and Michael M. Zavlanos, “A new one-point residual-feedback oracle for black-box learning and control,” *Automatica*, vol. 136, pp. 110006, 2022.

[41] Audrunas Gruslys, Rémi Munos, Ivo Danihelka, Marc Lanctot, and Alex Graves, “Memory-efficient backpropagation through time,” *Advances in Neural Information Processing Systems*, vol. 29, 2016.

[42] S. Bhatnagar, HL Prasad, and LA Prashanth, *Stochastic Recursive Algorithms for Optimization: Simultaneous Perturbation Methods*, Springer, 2013.